GENERATION OF FEMTOSECOND BUNCH TRAINS USING A LONGITUDINAL-TO-TRANSVERSE PHASE SPACE EXCHANGE TECHNIQUE*

Yin-e Sun[1], Philippe Piot[1,2]
[1]Accelerator Physics Center, Fermi National Accelerator Laboratory, Batavia IL 60510, USA
[2] Department of Physics, Northern Illinois University, DeKalb, IL 60115, USA

Abstract

We demonstrate analytically and via numerical simulations, how a longitudinal-to-transverse phase space manipulation can be used to produce a train of femtosecond electron bunches. The technique uses an incoming transversely-modulated electron beam obtained via destructive (e.g. using a multislits mask) methods. A transverse-to-longitudinal exchanger is used to map this transverse modulation into a temporal modulation. Limitation of the proposed method and scalability to the femtosecond regime are analyzed analytically and with the help of numerical simulation. Finally, a proof-of-principle experiment is discussed in the context of the Fermilab's A0 photoinjector.

INTRODUCTION

Modern applications of the accelerator often call for certain phase space distribution which sometimes can be achieved from the phase space manipulation within one or two degrees of freedom. For example, the production of comb bunches, i.e. a bunch consisting of a train of microbunches, could open the path toward compact light source operating in the super-radiant regime at a wavelength comparable or larger than the typical density modulation. The generation of such beams by shaping the photocathode drive laser of a photoemission electron source were explored via numerical simulations [1, 2]. An alternative method using an interceptive mask located in a dispersive section was experimentally demonstrated [3]. Each of these methods has its limitations: the method based on shaping the photocathode drive laser distribution is prone to space-charge effects which are prominent at low energy and wash out the impressed modulation; the other techniques have limited tunability. In this paper, we present a more general technique for tailoring the current profile to follow certain distribution: first the transverse beam profile is modulated using a mask in the beamline, then beam goes through a longitudinal-to-transverse phase space exchange [4, 5, 6], resulting in a longitudinally modulated beam.

* Work supported by by the Fermi Research Alliance, LLC under Contract No. DE-AC02-07CH11359 with the U.S. Department of Energy and by Northern Illinois University under Contract No. DE-AC02-76CH00300 with the U.S. Department of Energy.

THEORETICAL BACKGROUND

Our method is illustrated in Fig. 1: an incoming electron bunch is transversely intercepted by a mask with transmission function $T(x, y)$. The mask can have different patterns for various desired beam current profiles. In order to generate the comb bunches, we use a plate with multi vertical slits located upstream of an emittance exchanger beamline. The exchanger beamline consists of a dipole mode rf cavity flanked by two identical doglegs [5, 6]. The beam horizontal projection is mapped into the longitudinal (temporal) current density profile at the end of the emittance exchanger.

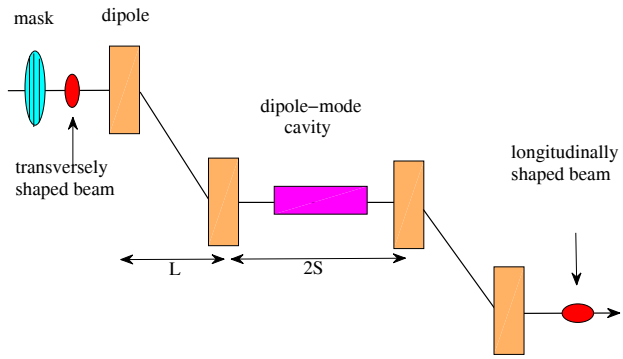

Figure 1: Overview of the proposed technique to produce relativistic electron bunch with arbitrary current profile.

A simple model based on the thin lens approximation for the transfer matrix associated to the dipole and cavity can be elaborated to give insights on the technique. In (x, x′, z, δ) phase space, the transfer matrix of a dogleg is

$$M_D = \begin{pmatrix} 1 & L & 0 & -L\alpha \\ 0 & 1 & 0 & 0 \\ 0 & -L\alpha & 1 & L\alpha^2 \\ 0 & 0 & 0 & 1 \end{pmatrix}, \quad (1)$$

where L is the drift distance between the two dipoles, and α is the bending angle. The matrix associated to a dipole-mode cavity with strength k is

$$M_C = \begin{pmatrix} 1 & 0 & 0 & 0 \\ 0 & 1 & k & 0 \\ 0 & 0 & 1 & 0 \\ k & 0 & 0 & 1 \end{pmatrix}. \quad (2)$$

Under the emittance exchange condition [5, 6], we have $k + \alpha L = 1$. The exchanger matrix simplifies to the block anti-diagonal form

$$\mathrm{M} = \begin{pmatrix} 0 & 0 & \frac{L+S}{\alpha L} & \alpha S \\ 0 & 0 & \frac{1}{\alpha L} & \alpha \\ \alpha & \alpha S & 0 & 0 \\ \frac{1}{\alpha L} & \frac{L+S}{\alpha L} & 0 & 0 \end{pmatrix}. \quad (3)$$

where $2S$ is the separation between the middle two dipoles (see Fig. 1). The final phase space coordinates relates to the initial ones via

$$\begin{pmatrix} x \\ x' \\ z \\ \delta \end{pmatrix}_f = \mathrm{M} \begin{pmatrix} x \\ x' \\ z \\ \delta \end{pmatrix}_i = \begin{pmatrix} \frac{L+S}{\alpha L} z_i + \alpha S \delta_i \\ \frac{1}{\alpha L} z_i + \alpha \delta_i \\ \alpha x_i + \alpha S x_i' \\ \frac{1}{\alpha L} x_i + \frac{L+S}{\alpha L} x_i' \end{pmatrix}. \quad (4)$$

From Eq. (4), we see that in order to replicate the initial x_i structure in the final coordinate z_f, we want the contribution to z_f from the term x_i' as small as possible. This can be done by (1) designing the beamline to minimize the bending angle α, and/or the drift space between the two center dipole magnets $2S$; (2) tuning the initial beam parameters such that the initial divergence of the beam, x_i', is as small as possible. For a given emittance, this means increasing the betatron function at the beam waist in (x, x′) phase space. It is also apparent that the correlation in an individual beamlet (for which the x_i is constants for an infinitely narrow slit in the multislit mask) in the longitudinal phase space at the end the exchange is given by

$$\frac{\Delta z}{\Delta \delta} = \frac{z_f - \alpha x_i}{\delta_f - x_i/\alpha L} = \frac{LS\alpha^2}{L+S} = \frac{M_{52}}{M_{62}}. \quad (5)$$

and is independent of the incoming Courant-Snyder parameters of the beam. A magnetic compressor with $R_{56} = -\frac{\Delta z}{\Delta \delta}$ can exploit the local correlation and further compresses the beamlets.

NUMERICAL SIMULATIONS

The emittance exchange beam line is composed of four rectangular magnets of length $L_b = 0.288$ m and bending angle $\alpha = 22.5\,^\circ$. The dipole mode cavity is the 3.9 GHz TM_{110} 5-cell copper cavity currently in operation at the A0 photoinjector in FermiLab [7]. The drift distances (see Fig. 1) are $L = 0.869$ m, $S = 0.400$ m.

The longitudinal chirp of the beam before it enters the emittance exchanger is chosen such to achieve the best possible emittance exchange as prescribed in Reference [8]; while the transverse Courant-Snyder parameters are tuned to obtain femtosecond bunch trains at the end of the exchanger; one set of initial conditions for the simulation is shown in Table 1.

The simulations are performed using GPT [9] and space charge is ignored for these simulations. A mask with vertical slits intercepts the beam in front of the emittance exchanger. The projection of the beam in the horizontal direction (x) is modulated; see the top picture in Fig. 2. At the end of the emittance exchanger, the beam intensity becomes modulated in the longitudinal direction (z) as a result of the swapping between the horizontal and longitudinal phase spaces. The modulation pattern is determined by the mask dimension as well as the lattice and the initial beam parameters, as shown in Eq. (4). Using the parameters shown in Table 1, the beam at the end of the emit-

Table 1: Parameters Prior to the Emittance Exchange

beam energy (MeV)	15
bunch charge (pC)	100
normalized horizontal emittance (μm)	1
normalized longitudinal emittance(μm)	27
horizontal beta function (m)	20
longitudinal chirp $\partial\delta/\partial z$ (m^{-1})	-4.5
rms bunch length (mm)	0.9
slit width (μm)	80
slit separation (μm)	300

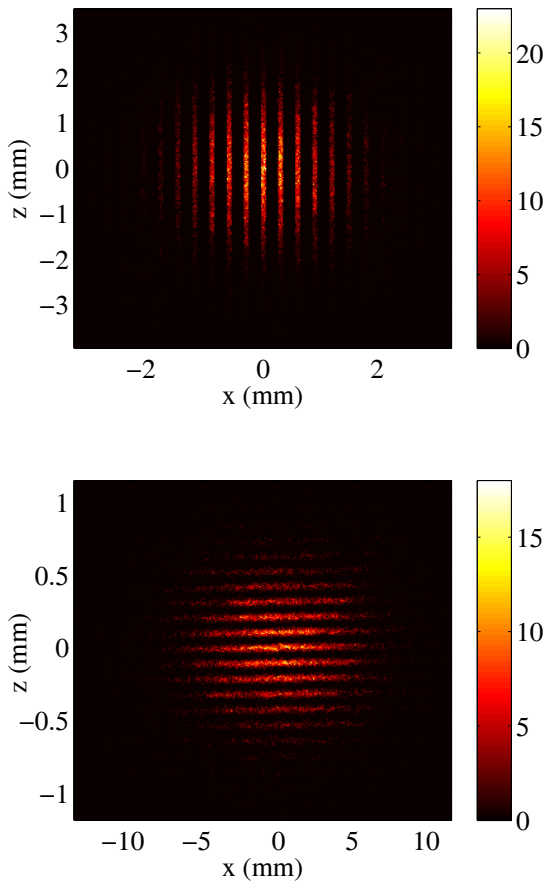

Figure 2: Beam projection in the x-z configuration space right after the mask (top) and at the end of the emittance exchanger (bottom).

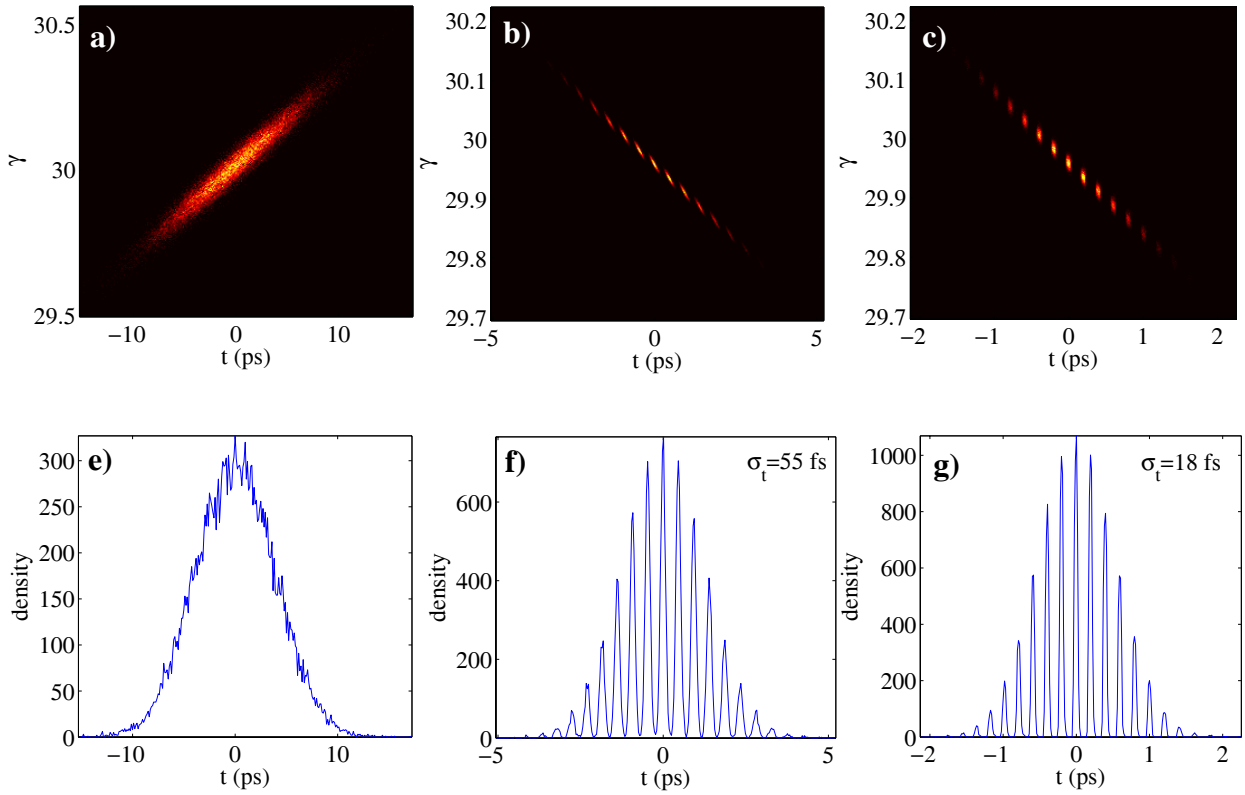

Figure 3: Longitudinal phase spaces (top) and their corresponding projections onto the time axis (bottom): a) & e) beam after the mask, at the entrance of the emittance exchanger; b) & f) beam at the end of the emittance exchanger; c) & g) beam downstream of a dogleg used to compress the beamlets. The bunch head corresponds to $t > 0$.

tance exchanger has a train of micro pulses with rms length around 55 fs. The separation between two neighbor micro pulses is about 350 fs; see Fig. 3 b) and f). The individual beamlets have a slope (correlation between energy and position) that is given by Eq. (5), which is different from the slope of the whole bunch train. In order to further compress the beamlet, one can use a two-dipole achromatic single dogleg compressor [10],which has the opposite R_{56} sign as a conventional four-dipole chicane magnetic compressor. The absolute value of R_{56} is given by Eq. (5). Upon the removal of the correlation in the longitudinal phase space within the beamlet, pulses with rms lengths of 18 fs and 120 fs separations are achieved; see Fig. 3 c) and g).

FUTURE PLANS

In our simulations, the input beam parameters and lattice used are very close to those available at the A0 photoinjector Laboratory, with the exception of the non-existing single dogleg compressor after the emittance exchanger. However it is not essential for a proof-of-principle experiment. We are therefore preparing an experiment at the A0 photoinjector aimed at demonstrating the concept presented in the preceding sections. A tungsten plate will be used to intercept the beam before the emittance exchanger and coherent transition radiation detected by a cryogenically-cooled InSb bolometer will provide information on the pulse structure downstream of the exchanger. The bolometer will be used to directly detect the radiation with a set of bandpass mesh filters and as part of a Michelson interferometer. The planned parametric studies include the variation of the width, separation and number of the slits.

REFERENCES

[1] M. Boscolo *et al.*, Nucl. Instrum. Methods A **577**, 409 (2007).

[2] Y. Li *et al.*, PRST-AB **11**, 080701 (2008).

[3] P. Muggli *et al.*, Phys. Rev. Lett. **101**, 054801 (2008).

[4] M. Cornacchia and P. Emma, PRST-AB **5**, 084001 (2002).

[5] K.-J. Kim and A. Sessler, AIP Conf. Proc. **821**, p. 115 (2006).

[6] P. Emma *et al.*, PRST-AB **9**, 100702 (2006).

[7] T. Koeth *et al.*, in Proc. of PAC 2007, pp. 3663 - 3665 (2007).

[8] Y.-E Sun *et al.*, in Proc. of PAC 2007, pp. 3441 - 3443 (2007).

[9] http://www.pulsar.nl/gpt.

[10] H. Wiedemann, "Particle Accelerator Physics I", second edition, p. 173, Spinger (1999).